Macromolecules

pubs.acs.org/Macromolecules Article

Synthesis of Narrowly Distributed α,ω-Bifunctionalized Conjugated Polymers

Jie Wang, Donglai Tian, Xuezheng Zhang, Huanghao Pan, Yun Ding, Guiyou Wang,* and Aiguo Hu*

Cite This: https://doi.org/10.1021/acs.macromol.3c00870 Read Online

ACCESS | Metrics & More | Article Recommendations | Supporting Information

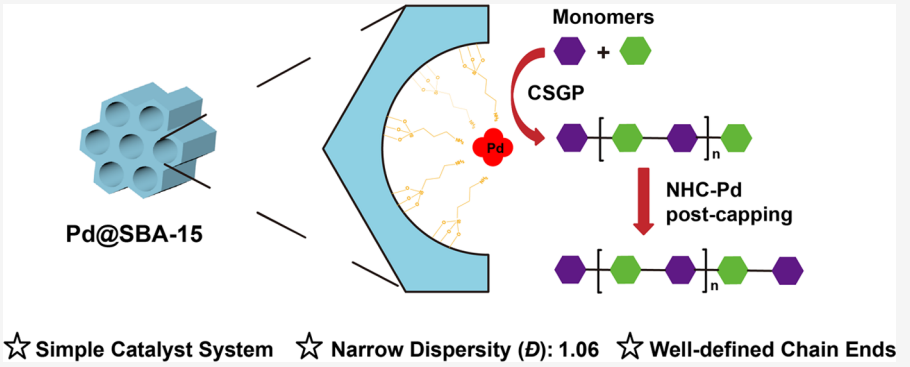

ABSTRACT: End-functional conjugated polymers are generally synthesized with stoichiometric-biased monomer combinations in conventional step growth polymerizations (SGPs), which lead to broad species distribution and difficult-to-control end functionality of the polymeric products due to the uncontrolled nature of the method employed. To overcome such disadvantages, a general controlled method was developed for the synthesis of narrowly distributed end-functional conjugated polymers with high-end functionality purity and a predefined molecular weight. This strategy relies on the spatial confinement effect of the nanoreactors, whereby polymeric species with higher molecular weight have a lower chance of further involvement in SGP. Numerical calculations on the kinetic equations demonstrated the formation of narrowly distributed polymers with a high degree of chain-end functionalization. Experimental results based on various analysis methods confirmed the controlled synthesis of bifunctionalized poly(*p*-phenylene)s with high-end functionality purity and low dispersity value down to 1.06.

1. INTRODUCTION

Conjugated polymers as a kind of intriguing materials have shown wide application scopes in fluorescent imaging and sensing,[1−4] organic light emission diodes (OLEDs),[5−9] organic photovoltaics (OPVs),[10−14] and organic field effect transistors (OFETs).[15−19] The π-conjugated backbones of conjugated polymers are mainly constructed with cross-coupling polymerizations through the step growth polymerization (SGP) pathway.[20] With the ever-increasing demand in improving the overall properties of conjugated polymers and pushing forward for industrial applications,[21] the precise control of the backbone, terminal structure, functionality, molecular weight, and molecular weight distribution (MWD, commonly measured as dispersity, $Đ$) of conjugated polymers is of essential importance. Due to the uncontrolled nature of SGP, the majority of conjugated polymers are synthesized with broad dispersity and/or difficult-to-control chain-end structures.[22−26] Resolving these issues would surely open a new era in the applications of functional conjugated polymer materials.

While great efforts have been devoted to modulating the main chain structure of conjugated polymers, like introducing various kinds of donor−acceptor (D−A) moieties, mitigating backbone defects, and controlling the head-to-tail patterns,[17,24,27,28] to name a few, one-pot or postpolymerization modification of side chains[29] and end groups also provide great possibilities to significantly enrich the structure and property of conjugated polymers.[30−36] Further derivatization at chain ends enables the synthesis of block copolymers for crystallization-driven self-assembly,[35−37] decorating nanoparticles for the fabrication of and layered hybrid nanocomposites. Hawker et al.[30] introduced perylene diimide (PDI) units at the chain ends of a donor−acceptor-type conjugated polymer PDPP2FT through a one-step strategy and found efficient charge transfer between PDI end groups and PDPP2FT main chains to reveal unique photophysical properties. Reynolds et al.[31] found that by introducing end-capping groups to a D−A-type conjugated

Received: May 5, 2023
Revised: July 8, 2023

copolymers, the obtained OFET devices showed around an order of magnitude higher charge-carrier mobility, demonstrating the importance of modulating end functionalities in controlling the polymer organization.

The end functionalization of conjugated polymers is typically accomplished by using stoichiometric imbalanced bifunctional monomers with the end-capping agents added simultaneously[30,32] or in a postpolymerization modification manner.[31] The uncontrolled nature of SGP leading to a relatively broad dispersity ($Đ$) of the conjugated polymers limits the possibility of further performance optimization. Turning to chain-growth polymerization methods like Grignard metathesis (GRIM)[38−40] reactions and catalyst transfer polycondensations (CTP)[35,41−44] indeed gives a narrow dispersity ($Đ$), well-defined backbone structure, and end groups. However, for the synthesis of conjugated polymers with rich D−A structures and side functionalities, cross-coupling polymerization in an SGP pathway is still the major method of choice. Therefore, developing a general strategy for the synthesis of conjugated polymers with controlled end-functional groups, predefined molecular weight, and narrow dispersity ($Đ$) is of significant importance. Recently, we developed a controlled step growth polymerization (CSGP) method by embedding the catalyst necessary for polymerization inside nanochannels and ushering the cross-coupling polymerizations in these confined environments. A variety of narrowly dispersed conjugated polymers were synthesized from either AB-type monomers or symmetrical AA+BB monomer combinations.[45] Herein, we extend this CSGP concept and develop a general kinetic model for the controlled synthesis of end-functionalized conjugated polymers. Numerical simulations and experimental results showed that broadly dispersed α,ω-bisfunctionalized conjugated polymers were formed through conventional SGP methods, while narrowly dispersed products with a $Đ$ value down to 1.06 were obtained in confined nanochannels.

2. RESULTS AND DISCUSSION

The species distribution in conventional SGP is solved with probabilistic methods developed by Flory and Carothers in 1930s[46,47] based on the "equal reactivity principle". While applied in polymerizations with AA+BB monomer combinations, a Carothers equation is typically used to correlate the theoretical number-average molecular weight (M_n) by employing the molar ratio (r) of two monomers and the conversion of the insufficient monomer (p_A) when the stoichiometry of AA monomer and BB monomer is biased.[48] The concentration of each species or $Đ$ value in these cases, however, has no analytical solution. The CSGP method developed previously in our group[45] was achieved based on a refined Flory model (RFM) for the polymerization of AB-type monomers with the introduction of a series of possibility coefficients (P). The P values gradually decreased with the increase of the length of the species, assuming that polymers with higher molecular weight have lower possibility to further get involved in SGP following a similar principle in gel permeation chromatography.[49] Numerical calculations based on RFM indeed gave well-controlled M_n and narrow dispersity ($Đ$), which was further confirmed by experimental results.

To come up with a general description of CSGP for end-functional polymers synthesized with stoichiometric imbalanced AA+BB monomers, the kinetic equations in the polymerization system[50] were rewritten (eqs 1−3), with the introduction of possibility coefficients P_i of the species with number i repeating units (for monomers, i and P_i equal 1 in definition). As shown in Table 1, species types "A_i" and "B_i"

Table 1. Types of Species Present in the SGP Simulation Progress

types of species	end groups	structure	constraint
A_i	a, a	a-$(A-B)_{i-1}$-A-a	$i > 0$
B_i	b, b	b-B-$(A-B)_{i-1}$-b	$i > 0$
M_i	b, a	b-B-$(A-B)_{i-1}$-AB-a	$i > 0$
A_0	a, a	a−a	
B_0	b, b	b−b	
M_0	a, b	a−b	

contain α,ω-functional groups of "a, a" and "b, b", respectively, while species type "M_i" contains "a" functional group at one end and "b" functional group at the other end. To simplify things, in eqs 1−6, the terms "A_i", "B_i", and "M_i" also refer to the concentration of each respective species. The rate constants k_{ab}, k_{am}, k_{bm}, and k_{mm} correspond to the reactions between "A" and "B", "A" and "M", "B" and "M", and "M" and "M", respectively. According to "Flory's principle", $k_{ab} = k_{am} = k_{bm} = k_{mm}$. Although the cases where these rate constants were not equal were reported lately in some specific SGPs,[50−54] the rate constant difference is negligible in the majority of SGPs. The P_i values are all of the same and equal to 1 in conventional SGPs, while they decrease with the increase of the length of the species when the SGPs take place exclusively in confined nanochannels similar to our previous work.[45] A reasonable assumption is made that species "A_i", "B_i", and "M_i" with the same number (i) of repeating units have the same P_i value. Numerical integrations of the kinetic equations were performed with MATLAB, and a truncation point (N), the largest species considered in the calculations,[55] was introduced to reduce the numerical complexity. For easier matrix language conversion in the MATLAB (MATLAB R2019a, MathWorks, Natick) simulation, we came up with the concept of "zeromers" (Table 1), introducing three imaginary species "A_0", "B_0", and "M_0", assuming they contain two end-functional groups and no repeating unit. They react the same way as monomers, oligomers, and polymers but do not change the length of any species. For example, when "A_0" reacts with "B_6", an "M_6" is generated. Since the initial "concentrations" of "zeromers" are set as 0, the introduction of them does not affect the calculational results. The concentrations of all of the species are calculated with loop functions written according to the kinetic equations, applying the *ode23tb* method in MATLAB (Supporting Information). The total concentration (C) and weight (W) of all of the species are calculated according to eqs 4 and 5. The M_n and weight-average molecular weight (M_w) are calculated based on their definition (eqs 7 and 8, where M_u is the molecular weight of the repeating unit). To simplify the matter, the end-functional groups were omitted in the calculation of M_n, M_w, and $Đ$.

$$\frac{dA_i}{dt} = 2k_{am}\sum_{j=0}^{i} A_jP_jM_{i-j}P_{i-j} - 2A_iP_i\left\{2k_{ab}\sum_{j=0}^{N} B_jP_j + k_{am}\sum_{j=0}^{N} M_jP_j\right\} \quad (1)$$

https://doi.org/10.1021/acs.macromol.3c00870
Macromolecules XXXX, XXX, XXX−XXX

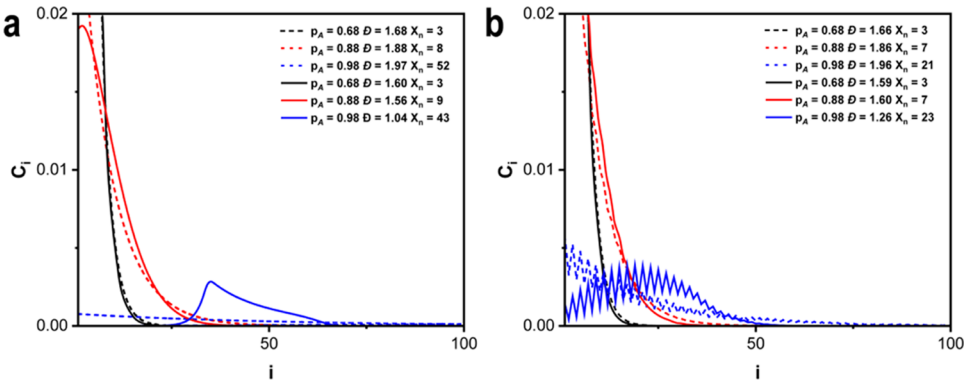

Figure 1. Species distribution curves of CSGP (solid line) and SGP (dashed line) at different conversions of the insufficient monomer (p_A): (a) r = 1 and (b) r = 1.05.

$$\frac{dB_i}{dt} = 2k_{bm}\sum_{j=0}^{i} B_jP_jM_{i-j}P_{i-j} - 2B_iP_i\left\{2k_{ab}\sum_{j=0}^{N} A_jP_j + k_{bm}\sum_{j=0}^{N} M_jP_j\right\} \quad (2)$$

$$\frac{dM_i}{dt} = 4k_{ab}\sum_{j=0}^{i} A_jP_jB_{i-j}P_{i-j} + k_{mm}\sum_{j=0}^{i} M_jP_jM_{i-j}P_{i-j} - 2M_iP_i\left\{k_{am}\sum_{j=0}^{N} A_jP_j + k_{bm}\sum_{j=0}^{N} B_jP_j + k_{mm}\sum_{j=0}^{N} M_jP_j\right\} \quad (3)$$

$$C = \sum_{i=1}^{N} (A_i + B_i + M_i) \quad (4)$$

$$W = \sum_{i=1}^{N} (iA_i + iB_i + iM_i) \quad (5)$$

$$Z = \sum_{i=1}^{N} (i^2A_i + i^2B_i + i^2M_i) \quad (6)$$

$$M_n = \frac{W}{C}M_u \quad (7)$$

$$M_w = \frac{Z}{W}M_u \quad (8)$$

This calculation method is indeed suitable for the simulation of all kinds of SGPs. For example, when the initial concentrations of "M_1" are set as 1, while all other species are set as 0, the kinetic equations will turn to the RFM model of the polymerization of AB-type monomers as reported in our previous work.[45] If the concentrations of "M_1" and "B_1" are set as 1 and a number smaller than 1, respectively, while the concentrations of all other species are set as 0, this method will be suitable to simulate the formation of polymers with two "b" end-functional groups from the homopolymerization of AB-type monomers in the presence of a small amount of BB-type end-capping agents. In this work, we focused on the synthesis of end-functional polymers with both ends terminated with "b" groups, starting from AA+BB monomer combinations, as these kinds of symmetrical molecules are readily available and are widely used in the majority of SGPs. The initial concentrations of "A_1" and "B_1" are set as 1 and a number corresponding to the monomer ratio ($r = B_1/A_1$), respectively, while all other species are set as 0. It should be noted that in the AA+BB polymerization system, the species with an odd number of repeating units contain all of the "A_i" and "B_i", while those with an even number of repeating units contain all of the "M_i".

The MATLAB simulations on the polymerization systems with various r values at low (68%), medium (88%), and high (98%) conversions (p_A) of insufficient monomers were performed on a laptop computer. A truncation point (N) of 500 is sufficient for most of the calculations and ensures that each calculation is complete in several minutes. The total weight (W) of all of the species was monitored, and if a significant amount of high molecular weight species were overlooked, a higher N number would be used. For the stoichiometric balanced polymerization (r = 1), as shown in Figure 1a, the species distribution in CSGP is comparable to that in conventional SGP at low conversion. With the increase of conversion, the Đ values in conventional SGP gradually increase, close to the theoretical maximum, 2. In a sharp comparison, the species distribution in CSGP gradually narrows to give rather low Đ values.

End-functional polymers are typically synthesized from stoichiometric-biased monomer combinations.[30−32] The polymerizations with slight excess of BB monomer were simulated in the same way as mentioned above. The results of r = 1.05 are shown in Figure 1b, and the results with other r values (1.10, 1.15, 1.20) are shown in Figures S1−S3. At high conversions (p_A), "sawtooth" curves appear in both conventional SGP and CSGP models, indicating that "B_i" are the dominant species in the mixture. For easy comparison of the purity of "b,b" end-functionalized polymers prepared through different strategies, an end-group "flaw" factor (F) is defined in eq 9. In conventional SGPs with r = 1, the F value gradually increases with the increase of conversion (p_A) and reaches an infinite number, 75%. It is reasonable that the molar ratio of "A", "M", and "B" reaches 1:2:1 at the end of polymerization, correlating to the percentage of the species without pure "b,b" end groups being 75%. With the increase of monomer ratio (r) from 1.05 to 1.20, the F value gradually decreases to 17% at high conversion (p_A = 0.98). Further decrease of the F value can be achieved at even higher conversions in longer

https://doi.org/10.1021/acs.macromol.3c00870
Macromolecules XXXX, XXX, XXX−XXX

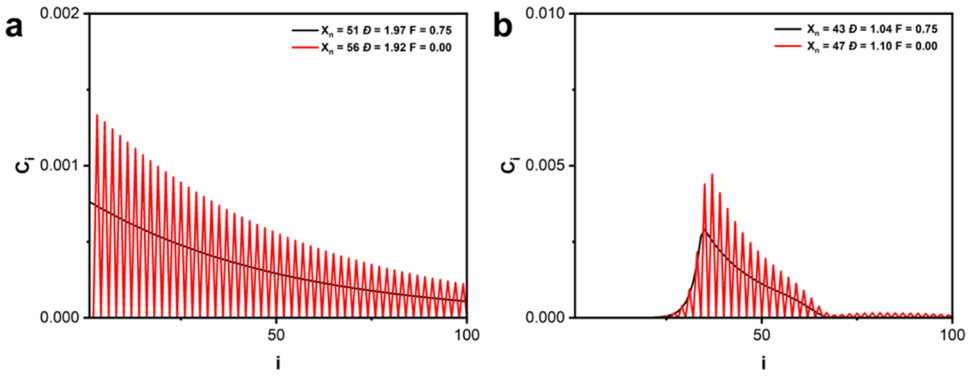

Figure 2. Species distribution curves of polymerization (r = 1) at p_A = 0.98 (black lines) and postpolymerization modification with 0.5 equiv of BB monomers (red lines). (a) SGP and (b) CSGP.

Scheme 1. Synthesis of Poly(*p*-phenylene)s and Postpolymerization Modification

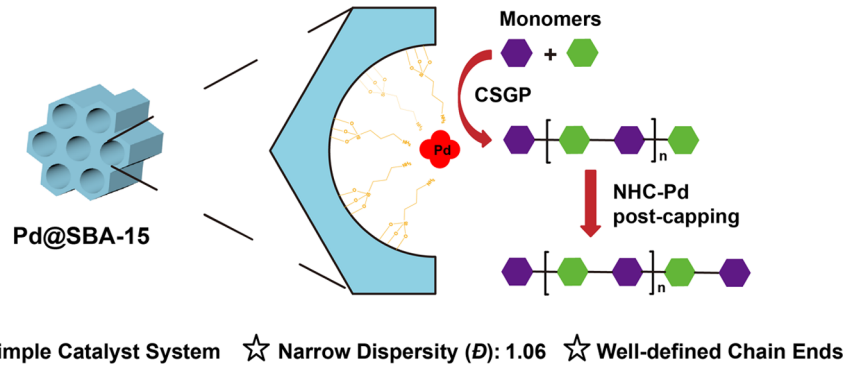

simulation (reaction) times. The trends of the F value change are similar in conventional SGP and CSGP models due to the fact that "Flory's principle" applies in both cases and the species with the same number of repeating units have the same possibility coefficient (P_i) in the CSGP model as defined above. Nevertheless, the end-functional polymers formed in the CSGP model always show much lower dispersity ($Đ$) than those in the conventional SGP model. At high monomer ratio (r), the species distribution is dictated by the presence of excess "b" functional groups; therefore, the curves obtained from conventional SGP and CSGP get more and more closer. Meanwhile, the theoretical M_n (or the number-average degree of polymerization, X_n) gradually decreases, as indicated in Carothers' equation and obtained in our MATLAB simulation

$$F = \frac{\sum_{i=1}^{N}(A_i + M_i)}{\sum_{i=1}^{N}(A_i + B_i + M_i)} \times 100\% \quad (9)$$

Postpolymerization modification is widely used to introduce end-functional groups after the SGPs are completed. The above simulation can also be used to simulate the species distribution in postpolymerization modification. Taking the modification of polymers with excess BB monomer as an example, the output matrix (corresponding to the concentrations of all of the species after polymerization) in MATLAB is modified by adding a number corresponding to the excess BB monomer to the "B_1" value and used as the input matrix and run the simulation again. Figure 2 shows the simulation results for the postpolymerization modification of polymers obtained at high conversion (r = 1, p_A = 0.98) with 0.5 equiv excess of BB monomer in conventional SGP and CSGP models. The addition of BB monomer does not change the contour profile of the species distribution curves very much but simply converts all of the "M" and "A" species to "B" species and changes the smooth curves to a sawtooth shape. It is encouraging that end-functional polymers with a predefined molecular weight (which can be controlled by varying the possibility coefficients), narrow dispersity ($Đ$), and free of chain-end impurity can be obtained by combining postpolymerization modification with the CSGP model.

In the experimental investigation, Suzuki−Miyaura polymerizations between 1,4-bis((2-ethylhexyl)oxy)-2,5-diiodobenzene (**1**, AA) and 1,4-benzenediboronic acid bis(pinacol) ester (**2**, BB) were chosen as the model reaction to study the controlled synthesis of end-functional poly(*p*-phenylene)s. In the conventional SGP mode, a highly reactive air- and moisture-stable palladium N-heterocyclic carbene complex (NHC-Pd)[56] was used as the homogeneous catalyst. In the CSGP mode, the Pd catalyst was embedded exclusively inside the channels of mesoporous silica SBA-15 (Pd@SBA-15) following similar procedures to differentiate the internal and external surfaces of these kinds of porous supports.[57−59] Free-standing sheet-like SBA-15 was chosen in this work, for their unique perpendicular orientated open channels with high diameter-to-length ratio[60] are beneficial for the diffusion of monomers and polymer chains. The porous properties of Pd@SBA-15 were characterized by nitrogen adsorption and desorption analysis (Figures S4 and S5), showing a narrowly ranged pore diameter of 11.8 nm. The Brunauer−Emmett−Teller (BET) surface area of Pd@SBA-15 is 418.5 $m^2\ g^{-1}$, similar to that of the SBA-15 support,[60] implying that the embedding of the Pd nanoparticles has negligible influence on the channel structure of the SBA-15 support. The amount of Pd species (0.43 wt %) was determined with inductively coupled plasma atomic

https://doi.org/10.1021/acs.macromol.3c00870
Macromolecules XXXX, XXX, XXX−XXX

emission spectroscopy (ICP-AES). The synthetic route and condition of the (end-functional) poly(*p*-phenylene)s are illustrated in Scheme 1.

The polymerization in the conventional SGP mode or CSGP mode was conducted in the presence of 1% Pd as either homogeneous or heterogeneous catalyst at different monomer ratios (r). All of the reactions were performed in *N*,*N*-dimethylacetamide (DMAc) at elevated temperature with cesium carbonate (Cs_2CO_3) as the base. Due to the localization of catalysts on the porous support can result in a lower probability of monomer−catalyst collisions, leading to slower reactions, highly reactive aryl iodide was selected as the monomer to facilitate the polymerization. Meanwhile, polar aprotic solvents, such as DMAc, that have beneficial effects on the rate-limiting step of the Suzuki coupling reaction were selected to promote a reasonable reaction rate in this heterogeneous polymerization system. The M_n and $Đ$ values were directly measured with gel permeation chromatography (GPC) after the polymerizations were completed, and all of the results are listed in Table 2 and Figures S7 and S8. The integration for M_n and $Đ$ was selected, excluding the peaks corresponding to monomers and residual solvent. For the polymerizations in the conventional SGP mode at low monomer ratios, the reactions were stopped before a significant amount of high polymers precipitated out. Similar to the simulation results, the dispersity ($Đ$) of the polymers obtained in confined nanoreactors is much narrower than those obtained in conventional homogeneous catalytic polymerizations. For example, when r = 1, the M_n values of the polymers obtained are similar to each other (entry 1 vs entry 6), while the $Đ$ values are significantly different (1.10 vs 1.81). When the r value increases from 1.00 to 1.20, the M_n gradually decreases in both conventional SGP and CSGP systems, and the $Đ$ values move closer to each other, similar to the trend obtained in the above simulations.

Table 2. Suzuki Polymerization of Monomers 1 and 2[a]

entry	polymer	[2]/[1]	catalyst	M_n[b] (kDa)	M_w/M_n[b]
1	**P1**	1.00	Pd@SBA-15	6.5	1.10
2	**P2**	1.05	Pd@SBA-15	5.7	1.20
3	**P3**	1.10	Pd@SBA-15	5.6	1.43
4	**P4**	1.15	Pd@SBA-15	4.4	1.46
5	**P5**	1.20	Pd@SBA-15	3.9	1.57
6	**P6**	1.00	NHC-Pd	7.4	1.81
7	**P7**	1.05	NHC-Pd	5.1	1.74
8	**P8**	1.10	NHC-Pd	4.9	1.71
9	**P9**	1.15	NHC-Pd	3.6	1.68
10	**P10**	1.20	NHC-Pd	3.4	1.47
11	**P11**[c]	/	NHC-Pd	7.1	1.06

[a]Polymerizations were carried out in the presence of 1% mol of Pd and 3 equiv of Cs_2CO_3 in DMAc at 80 °C ($[\mathbf{1}]_0$ = 0.1 M) for 5 d except for those entries noted in the main text. [b]Determined by GPC using polystyrene standards. [c]After the synthesis of **P1** was completed, the reaction system was added with 0.5 equiv of **2** and 1% mol of NHC-Pd catalyst and further reacted for 24 h.

As suggested by the simulation results above, combining postpolymerization modification with CSGP is essential for producing end-functional polymers with predefined and narrowly dispersed molecular weight. To this end, poly(*p*-phenylene) with both ends terminated with boronate groups was synthesized according to this strategy. Briefly, to the **P1** polymer synthesized with the Pd@SBA-15 catalyst at a 1:1 monomer ratio, 0.5 equiv of monomer **2** was added together with the NHC-Pd catalyst to facilitate the end-group modification process. As shown in Table 2 (entry 11), a polymer (**P11**) with M_n slightly higher than that of **P1** was obtained, suggesting the incorporation of BB monomer to "*A*" and "*M*" species and conversion of them to "*B*" species with longer repeating units. Encouragingly, the dispersity ($Đ$) of **P11** is extremely narrow (1.06), which fulfills the strict criterion in constructing structural regulated block copolymers[35−37] for more challenging applications.

The ^{1}H NMR spectra (Figure S6) of these (end-functional) poly(*p*-phenylene)s are similar to each other. The multiple peaks around 7.00 and 7.60 ppm relate to the aromatic protons in internal "*A*" and "*B*" moieties, respectively. The signal at 7.16 ppm belongs to the protons at the ortho-positions of iodine terminals (the aromatic protons in residual monomer **1** also show up here). The peak at 7.81 ppm indicates the presence of the residual monomer **2**. The multiplets at the far left side of the spectra correspond to the protons of the benzene ring with terminal pinacol boronate groups. A comparison of the spectra of **P11** with **P1** in Figure 3 indicates that the signal at 7.16 ppm disappeared completely, suggesting the formation of α,ω-bisboronate end-capped poly(*p*-phenylene) with a zero "*F*" value, the same as the simulation result in Figure 2b. End-group analysis on the NMR spectrum of **P11** showed an M_n of around 4.5 kDa, slightly lower than that obtained from the GPC analysis, corresponding to a poly(*p*-phenylene) with about 23 *p*-phenylene units and two pinacol boronate groups.

Matrix-assisted laser desorption ionization time-of-flight (MALDI-TOF) mass spectrometry is generally used to characterize the species in the polymeric products. It is especially useful in identifying end groups in polymers. MALDI-TOF MS spectra of **P1** and **P11** are shown in Figure 4. The peaks of m/z values at 1833.8, 2242.1 and 2650.3, 3058.6 of **P1** (marked in yellow) correspond to the polymers with bis-iodine terminal groups and four, five, six, and seven "*A*−*B*" repeating units (molecular weight of 408.3), respectively. The spectrum also shows the polymer chains with double pinacol boronate end groups (marked in blue and black). After the postpolymerization modification with monomer **2**, the MALDI-TOF MS spectrum of **P11** shows only the peaks related to double pinacol boronate end groups, and no diiodine-terminated species is found, further confirming the formation of α,ω-bisboronate end-capped poly(*p*-phenylene) with high-end-functional group purity.

3. CONCLUSIONS

In summary, a method for the controlled synthesis of α,ω-bifunctionalized polymers from AA+BB monomer combinations was established theoretically and experimentally. In theory, the kinetic equations in conventional SGP were modified with the introduction of a series of possibility coefficient (P_i) that correlate to the chances of these species further getting involved in SGP. Numerical simulations with MATLAB showed that end-functional polymers formed in the CSGP model were more narrowly dispersed, and combining postpolymerization modification strategy with CSGP gave α,ω-bifunctionalized polymers with predefined molecular weight, narrow dispersity, and high-end functionality purity. In experimental verification, a Suzuki−Miyaura polymerization was chosen as the model reaction to synthesize bisboronate-

https://doi.org/10.1021/acs.macromol.3c00870
Macromolecules XXXX, XXX, XXX−XXX

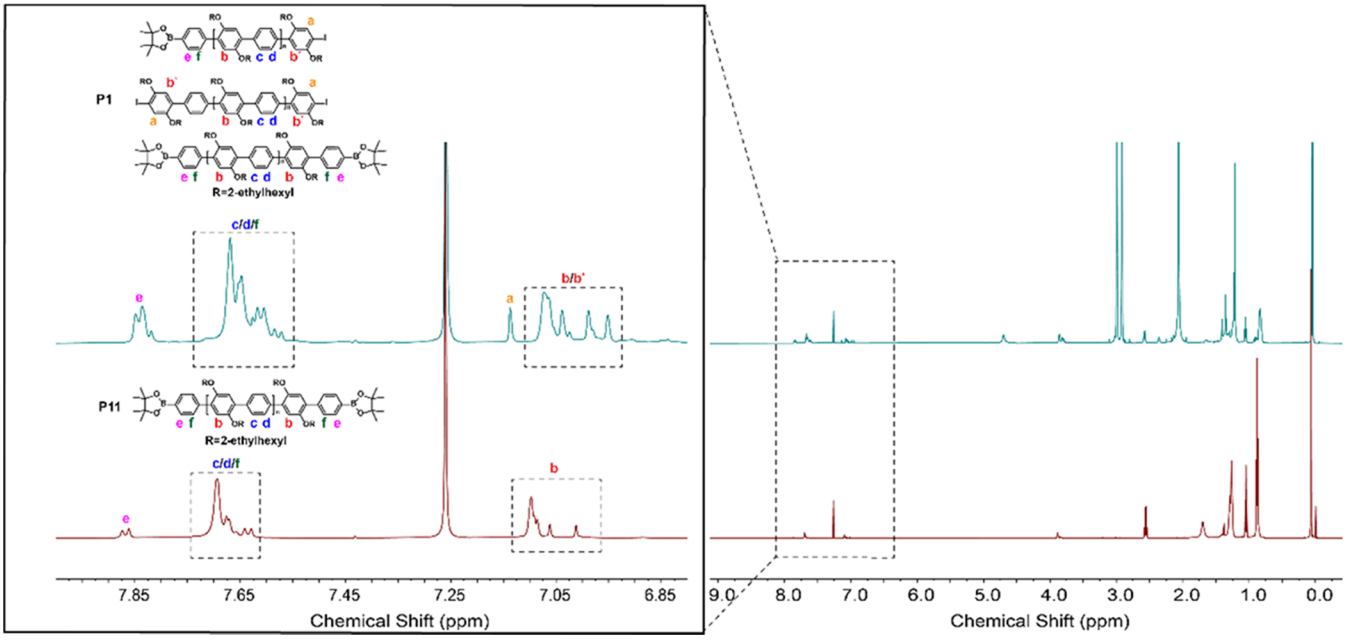

Figure 3. ^{1}H NMR spectra of **P1** and **P11** in $CDCl_3$.

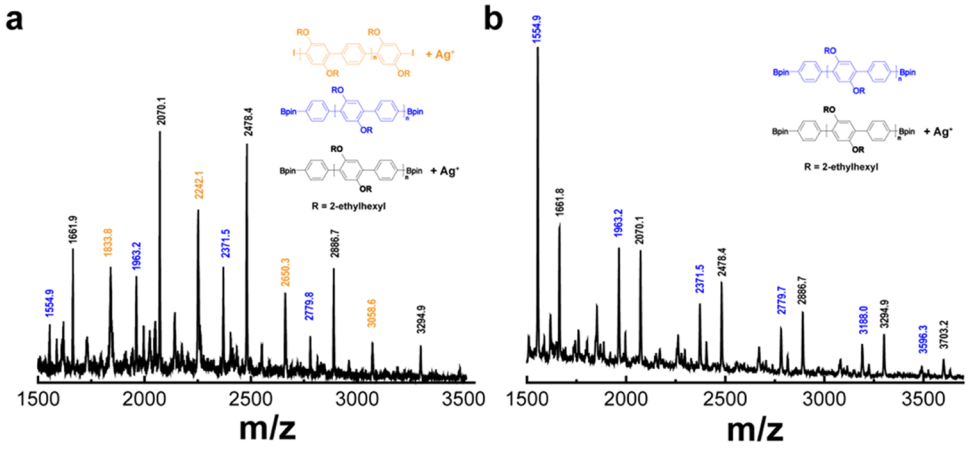

Figure 4. MALDI-TOF MS spectra of **P1** and **P11**.

terminated poly(*p*-phenylene)s in a controlled manner. The CSGP mode was achieved with all of the catalysts embedded in the nanochannels of the SBA-15 support, and conventional SGPs were performed with a highly reactive homogeneous catalyst for comparison. Through GPC, NMR, and MALDI-TOF analysis on the products, it is confirmed that conjugated polymers with high-end-functionalized efficiency and narrow dispersity were obtained. The controlled synthesis of end-functional conjugated polymers would benefit the improvement of the performances of conjugated polymer in future applications.

■ ASSOCIATED CONTENT

Supporting Information

The Supporting Information is available free of charge at https://pubs.acs.org/doi/10.1021/acs.macromol.3c00870.

Materials and testing method; synthesis method of monomers and polymers; numerical simulation method; and porous property of the catalyst, NMR spectra, and GPC curves of polymers (PDF)

■ AUTHOR INFORMATION

Corresponding Authors

Guiyou Wang − *Shanghai Key Laboratory of Advanced Polymeric Materials, School of Materials Science and Engineering, East China University of Science and Technology, Shanghai 200237, China;* orcid.org/0000-0001-9863-1465; Phone: +86-021-64252271; Email: guiyouwang@ecust.edu.cn

Aiguo Hu − *Shanghai Key Laboratory of Advanced Polymeric Materials, School of Materials Science and Engineering, East China University of Science and Technology, Shanghai 200237, China;* orcid.org/0000-0003-0456-7269; Phone: +86-021-64253037; Email: hagmhsn@ecust.edu.cn

Authors

Jie Wang − *Shanghai Key Laboratory of Advanced Polymeric Materials, School of Materials Science and Engineering, East China University of Science and Technology, Shanghai 200237, China*

https://doi.org/10.1021/acs.macromol.3c00870
Macromolecules XXXX, XXX, XXX−XXX

Donglai Tian − *Shanghai Key Laboratory of Advanced Polymeric Materials, School of Materials Science and Engineering, East China University of Science and Technology, Shanghai 200237, China*

Xuezheng Zhang − *Shanghai Key Laboratory of Advanced Polymeric Materials, School of Materials Science and Engineering, East China University of Science and Technology, Shanghai 200237, China*

Huanghao Pan − *Shanghai Key Laboratory of Advanced Polymeric Materials, School of Materials Science and Engineering, East China University of Science and Technology, Shanghai 200237, China*

Yun Ding − *Shanghai Key Laboratory of Advanced Polymeric Materials, School of Materials Science and Engineering, East China University of Science and Technology, Shanghai 200237, China;* orcid.org/0000-0002-7012-5621

Complete contact information is available at: https://pubs.acs.org/10.1021/acs.macromol.3c00870

Author Contributions

The manuscript was written through contributions of all authors. All authors have given approval to the final version of the manuscript.

Notes

The authors declare no competing financial interest.

■ ACKNOWLEDGMENTS

The authors gratefully acknowledge the financial support from the National Natural Science Foundation of China (22171083) and the Shanghai Leading Academic Discipline Project (B502). A.H. thanks the "Eastern Scholar Professorship" for support from Shanghai local government.

■ REFERENCES

(1) Freudenberg, J.; Jänsch, D.; Hinkel, F.; Bunz, U. H. F. Immobilization Strategies for Organic Semiconducting Conjugated Polymers. *Chem. Rev.* **2018**, *118* (11), 5598−5689.

(2) Zhu, C.; Liu, L.; Yang, Q.; Lv, F.; Wang, S. Water-Soluble Conjugated Polymers for Imaging, Diagnosis, and Therapy. *Chem. Rev.* **2012**, *112* (8), 4687−4735.

(3) Peters, M.; Zaquen, N.; D'Olieslaeger, L.; Bové, H.; Vanderzande, D.; Hellings, N.; Junkers, T.; Ethirajan, A. PPV-Based Conjugated Polymer Nanoparticles as a Versatile Bioimaging Probe: A Closer Look at the Inherent Optical Properties and Nanoparticle−Cell Interactions. *Biomacromolecules* **2016**, *17* (8), 2562−2571.

(4) Feng, G.; Liu, J.; Geng, J.; Liu, B. Conjugated polymer microparticles for selective cancer cell image-guided photothermal therapy. *J. Mater. Chem. B* **2015**, *3* (6), 1135−1141.

(5) Xu, Y.; Hai, G.; Xu, H.; Zhang, H.; Zuo, Z.; Zhang, Q.; Xia, R.; Sun, C.; Castro-Smirnov, J.; Sousaraei, A.; Casado, S.; Osorio, M. R.; Granados, D.; Rodriguez, I.; Cabanillas-Gonzalez, J. Efficient Optical Gain from Near-Infrared Polymer Lasers Based on Poly[N-9′-heptadecanyl-2,7-carbazole-alt-5,5-(4′,7′-di-2-thienyl-2′,1′,3′-benzothiadiazole)]. *Adv. Opt. Mater.* **2018**, *6* (15), No. 1800263.

(6) Samanta, S. K.; Kumar, G. S.; Ghorai, U. K.; Scherf, U.; Acharya, S.; Bhattacharya, S. Synthesis of High Molecular Weight 1,4-Polynaphthalene for Solution-Processed True Color Blue Light Emitting Diode. *Macromolecules* **2018**, *51* (20), 8324−8329.

(7) Zalar, P.; Henson, Z. B.; Welch, G. C.; Bazan, G. C.; Nguyen, T. Q. Color Tuning in Polymer Light-Emitting Diodes with Lewis Acids. *Angew. Chem., Int. Ed.* **2012**, *51* (30), 7495−7498.

(8) Ichige, A.; Saito, H.; Kuwabara, J.; Yasuda, T.; Choi, J.-C.; Kanbara, T. Facile Synthesis of Thienopyrroledione-Based π-Conjugated Polymers via Direct Arylation Polycondensation under Aerobic Conditions. *Macromolecules* **2018**, *51* (17), 6782−6788.

(9) Bhuvana, K. P.; Bensingh, R. J.; Kader, M. A.; Nayak, S. K. Polymer Light Emitting Diodes: Materials, Technology and Device. *Polym.-Plast. Technol. Eng.* **2018**, *57* (17), 1784−1800.

(10) Kim, H.; Lee, B. H.; Lee, K. C.; Kim, G.; Yu, J. Y.; Kim, N.; Lee, S. H.; Lee, K. Role of the Side Chain in the Phase Segregation of Polymer:Fullerene Bulk Heterojunction Composites. *Adv. Energy Mater.* **2013**, *3* (12), 1575−1580.

(11) Liu, C.; Wang, K.; Gong, X.; Heeger, A. J. Low bandgap semiconducting polymers for polymeric photovoltaics. *Chem. Soc. Rev.* **2016**, *45* (17), 4825−4846.

(12) Wang, G.; Melkonyan, F. S.; Facchetti, A.; Marks, T. J. All-Polymer Solar Cells: Recent Progress, Challenges, and Prospects. *Angew. Chem., Int. Ed.* **2019**, *58* (13), 4129−4142.

(13) Murakami, H.; Kobayashi, K.; Suzuki, K.; Yasuda, T.; Kanbara, T.; Kuwabara, J. Synthesis of Azine-Based Conjugated Polymers by Metal-Free Dehydration Polycondensation and Characterization of Their Physical Properties. *Macromolecules* **2021**, *54* (24), 11281−11288.

(14) Lo, C. K.; Gautam, B. R.; Selter, P.; Zheng, Z.; Oosterhout, S. D.; Constantinou, I.; Knitsch, R.; Wolfe, R. M. W.; Yi, X.; Brédas, J.-L.; So, F.; Toney, M. F.; Coropceanu, V.; Hansen, M. R.; Gundogdu, K.; Reynolds, J. R. Every Atom Counts: Elucidating the Fundamental Impact of Structural Change in Conjugated Polymers for Organic Photovoltaics. *Chem. Mater.* **2018**, *30* (9), 2995−3009.

(15) Klauk, H. Organic thin-film transistors. *Chem. Soc. Rev.* **2010**, *39* (7), 2643−2666.

(16) Liu, Q.; Kumagai, S.; Manzhos, S.; Chen, Y.; Angunawela, I.; Nahid, M. M.; Feron, K.; Bottle, S. E.; Bell, J.; Ade, H.; Takeya, J.; Sonar, P. Synergistic Use of Pyridine and Selenophene in a Diketopyrrolopyrrole-Based Conjugated Polymer Enhances the Electron Mobility in Organic Transistors. *Adv. Funct. Mater.* **2020**, *30* (34), No. 2000489.

(17) Xu, J.; Wu, H.-C.; Mun, J.; Ning, R.; Wang, W.; Wang, G.-J. N.; Nikzad, S.; Yan, H.; Gu, X.; Luo, S.; Zhou, D.; Tok, J. B.-H.; Bao, Z. Tuning Conjugated Polymer Chain Packing for Stretchable Semiconductors. *Adv. Mater.* **2022**, *34* (22), No. 2104747.

(18) Luo, L. X.; Huang, W. N.; Yang, C. L.; Zhang, J.; Zhang, Q. C. Recent advances on pi-conjugated polymers as active elements in high performance organic field-effect transistors. *Front. Phys.* **2021**, *16* (3), No. 33500, DOI: 10.1007/s11467-020-1045-6.

(19) Sui, Y.; Deng, Y.; Du, T.; Shi, Y.; Geng, Y. Design strategies of n-type conjugated polymers for organic thin-film transistors. *Mater. Chem. Front.* **2019**, *3* (10), 1932−1951.

(20) Flory, P. J. *Principles of Polymer Chemistry*; Cornell Univ. Press: Ithaca, NY, 1953; p 688.

(21) Prechtl, T.; Müllen, K.Precision and Purity of Conjugated Polymers − To be Ensured Before Processing. In *Solution-Processable Components for Organic Electronic Devices*; Wiley-VCH Verlag GmbH & Co. KGaA, 2019; pp 1−55. DOI: 10.1002/9783527813872.ch1.

(22) Sui, Y.; Shi, Y.; Deng, Y.; Li, R.; Bai, J.; Wang, Z.; Dang, Y.; Han, Y.; Kirby, N.; Ye, L.; Geng, Y. Direct Arylation Polycondensation of Chlorinated Thiophene Derivatives to High-Mobility Conjugated Polymers. *Macromolecules* **2020**, *53* (22), 10147−10154.

(23) Ye, L.; Thompson, B. C. Improving the efficiency and sustainability of catalysts for direct arylation polymerization (DArP). *J. Polym. Sci.* **2022**, *60* (3), 393−428.

(24) Kleybolte, M. E.; Vagin, S. I.; Rieger, B. High-Molecular-Weight Bisalkoxy-Substituted Poly(para)phenylenes by Kumada Polymerization. *Macromolecules* **2022**, *55* (13), 5361−5370.

(25) Collier, G. S.; Wilkins, R.; Tomlinson, A. L.; Reynolds, J. R. Exploring Isomeric Effects on Optical and Electrochemical Properties of Red/Orange Electrochromic Polymers. *Macromolecules* **2021**, *54* (4), 1677−1692.

(26) Hwang, K.; Lee, M.-H.; Kim, J.; Kim, Y.-J.; Kim, Y.; Hwang, H.; Kim, I.-B.; Kim, D.-Y. 3,4-Ethylenedioxythiophene-Based Isomer-Free Quinoidal Building Block and Conjugated Polymers for Organic Field-Effect Transistors. *Macromolecules* **2020**, *53* (6), 1977−1987.

(27) Ni, Z.; Wang, H.; Dong, H.; Dang, Y.; Zhao, Q.; Zhang, X.; Hu, W. Mesopolymer synthesis by ligand-modulated direct arylation

polycondensation towards n-type and ambipolar conjugated systems. *Nat. Chem.* **2019**, *11* (3), 271−277.
(28) Liu, Y. Y.; Li, B. J.; Xiang, Z. H. Pathways towards Boosting Solar-Driven Hydrogen Evolution of Conjugated Polymers. *Small* **2021**, *17* (34), No. 2007576.
(29) Ponder, J. F.; Gregory, S. A.; Atassi, A.; Menon, A. K.; Lang, A. W.; Savagian, L. R.; Reynolds, J. R.; Yee, S. K. Significant Enhancement of the Electrical Conductivity of Conjugated Polymers by Post-Processing Side Chain Removal. *J. Am. Chem. Soc.* **2022**, *144* (3), 1351−1360.
(30) Robb, M. J.; Montarnal, D.; Eisenmenger, N. D.; Ku, S. Y.; Chabinyc, M. L.; Hawker, C. J. A One-Step Strategy for End-Functionalized Donor-Acceptor Conjugated Polymers. *Macromolecules* **2013**, *46* (16), 6431−6438.
(31) Koldemir, U.; Puniredd, S. R.; Wagner, M.; Tongay, S.; McCarley, T. D.; Kamenov, G. D.; Müllen, K.; Pisula, W.; Reynolds, J. R. End Capping Does Matter: Enhanced Order and Charge Transport in Conjugated Donor−Acceptor Polymers. *Macromolecules* **2015**, *48* (18), 6369−6377.
(32) Harris, J. D.; Carter, K. R. A one-pot strategy to improve end-capping efficacy in Stille poly-condensations. *Polym. Chem.* **2018**, *9* (9), 1132−1138.
(33) Mondal, T.; Ghosh, S. A remarkable impact of a minor structural variation in the chain-end on the hierarchical self-assembly of a polymeric foldamer. *Polym. Chem.* **2016**, *7* (44), 6735−6743.
(34) Inagaki, S.; Higashihara, T. Synthesis of an ABC triblock copolymer by a bilateral Click reaction using α,ω-bifunctionalized poly(3-hexylthiophene) as an inner segment. *Polym. Chem.* **2022**, *13* (24), 3613−3618.
(35) Delabie, J.; De Winter, J.; Deschaume, O.; Bartic, C.; Gerbaux, P.; Verbiest, T.; Koeckelberghs, G. Development of a Layered Hybrid Nanocomposite Material Using α,ω-Bifunctionalized Polythiophenes. *Macromolecules* **2020**, *53* (24), 11098−11105.
(36) Nomura, K.; Haque, T.; Onuma, T.; Hajjaj, F.; Asano, M. S.; Inagaki, A. Precise One-Pot Synthesis of End-Functionalized Conjugated Multi-Block Copolymers via Combined Olefin Metathesis and Wittig-type Coupling. *Macromolecules* **2013**, *46* (24), 9563−9574.
(37) Ellis, C. E.; Garcia-Hernandez, J. D.; Manners, I. Scalable and Uniform Length-Tunable Biodegradable Block Copolymer Nanofibers with a Polycarbonate Core via Living Polymerization-Induced Crystallization-Driven Self-assembly. *J. Am. Chem. Soc.* **2022**, *144* (44), 20525−20538.
(38) Jeffries-El, M.; Sauvé, G.; McCullough, R. D. Facile Synthesis of End-Functionalized Regioregular Poly(3-alkylthiophene)s via Modified Grignard Metathesis Reaction. *Macromolecules* **2005**, *38* (25), 10346−10352.
(39) Zhai, D.; Zhu, M.; Chen, S.; Yin, Y.; Shang, X.; Li, L.; Zhou, G.; Peng, J. Effect of Block Sequence in All-Conjugated Triblock Copoly(3-alkylthiophene)s on Control of the Crystallization and Field-Effect Mobility. *Macromolecules* **2020**, *53* (14), 5775−5786.
(40) Yamamoto, T.; Hosokawa, M.; Nakamura, M.; Sato, S.-i.; Isono, T.; Tajima, K.; Satoh, T.; Sato, M.; Tezuka, Y.; Saeki, A.; Kikkawa, Y. Synthesis, Isolation, and Properties of All Head-to-Tail Cyclic Poly(3-hexylthiophene): Fully Delocalized Exciton over the Defect-Free Ring Polymer. *Macromolecules* **2018**, *51* (22), 9284−9293.
(41) Ye, S.; Cheng, S.; Pollit, A. A.; Forbes, M. W.; Seferos, D. S. Isolation of Living Conjugated Polymer Chains. *J. Am. Chem. Soc.* **2020**, *142* (25), 11244−11251.
(42) Yokozawa, T.; Ohta, Y. Transformation of Step-Growth Polymerization into Living Chain-Growth Polymerization. *Chem. Rev.* **2016**, *116* (4), 1950−1968.
(43) Kim, H.; Lee, J.; Kim, T.; Cho, M.; Choi, T.-L. Precision Synthesis of Various Low-Bandgap Donor−Acceptor Alternating Conjugated Polymers via Living Suzuki−Miyaura Catalyst-Transfer Polymerization. *Angew. Chem., Int. Ed.* **2022**, *61* (31), No. e202205828.
(44) Yang, H.-S.; Choi, H.-N.; Lee, I.-H. Recent progress on end-group chemistry of conjugated polymers based on Suzuki-Miyaura catalyst-transfer polymerization. *Giant* **2023**, *14*, No. 100152.
(45) Wu, Y.; Ding, M.; Wang, J.; Zhao, B.; Wu, Z.; Zhao, P.; Tian, D.; Ding, Y.; Hu, A. Controlled Step-Growth Polymerization. *CCS Chem.* **2020**, *2* (2), 64−70.
(46) Carothers, W. H. Polymers and polyfunctionality. *Trans. Faraday Soc.* **1936**, *32* (0), 39−49.
(47) Flory, P. J. Molecular Size Distribution in Linear Condensation Polymers1. *J. Am. Chem. Soc.* **1936**, *58* (10), 1877−1885.
(48) Hamaide, T.; Holl, Y.; Fontaine, L.; Six, J.-L.; Soldera, A. Teaching Polymer Chemistry: Revisiting the Syllabus. *Open J. Polym. Chem.* **2012**, *02* (04), 132−143.
(49) de Gennes, P.-G. Flexible Polymers in Nanopores. In *Polymers in Confined Environments*; Granick, S.; Binder, K.; de Gennes, P. G.; Giannelis, E. P.; Grest, G. S.; Hervet, H.; Krishnamoorti, R.; Léger, L.; Manias, E.; Raphaël, E.; Wang, S. Q., Eds.; Springer Berlin Heidelberg: Berlin, Heidelberg, 1999; pp 91−105.
(50) Romero-Hernández, J. E.; Cruz-Rosado, A.; Vivaldo-Lima, E.; Palacios-Alquisira, J.; Zolotukhin, M. G. Analysis of the Competition between Cyclization and Linear Chain Growth in Kinetically Controlled A(2) + B(2)Step-Growth Polymerizations Using Modeling Tools. *Macromol. Theory Simul.* **2020**, *29* (6), 2000050.
(51) Cruz, A. R.; Hernandez, M. C. G.; Guzmán-Gutiérrez, M. T.; Zolotukhin, M. G.; Fomine, S.; Morales, S. L.; Kricheldorf, H.; Wilks, E. S.; Cárdenas, J.; Salmón, M. Precision Synthesis of Narrow Polydispersity, Ultrahigh Molecular Weight Linear Aromatic Polymers by A2 + B2 Nonstoichiometric Step-Selective Polymerization. *Macromolecules* **2012**, *45* (17), 6774−6780.
(52) Zhang, L.; Ren, X.; Zhang, Y.; Zhang, K. Step-Growth Polymerization Method for Ultrahigh Molecular Weight Polymers. *ACS Macro. Lett.* **2019**, *8* (8), 948−954.
(53) Cruz-Rosado, A.; Romero-Hernández, J. E.; Ríos-López, M.; López-Morales, S.; Cedillo, G.; Ríos-Ruiz, L. M.; Cetina-Mancilla, E.; Palacios-Alquisira, J.; Zolotukhin, M. G.; Vivaldo-Lima, E. Molecular weight development in the superacid-catalyzed polyhydroxyalkylation of 1-propylisatin and biphenyl at stoichiometric conditions. *Polymer* **2022**, *243*, No. 124616.
(54) Matsumoto, K.; Fukui, C.; Shoji, R.; Jikei, M. Synthesis of aromatic polyketones by nonstoichiometric Friedel−Crafts polycondensation using AlCl3. *Polym. Chem.* **2020**, *11* (26), 4221−4227.
(55) Gordon, M.; Temple, W. B. Ring-chain competition kinetics in linear polymers. *Makromol. Chem.* **1972**, *152* (1), 277−289.
(56) O'Brien, C. J.; Kantchev, E. A. B.; Valente, C.; Hadei, N.; Chass, G. A.; Lough, A.; Hopkinson, A. C.; Organ, M. G. Easily Prepared Air- and Moisture-Stable Pd−NHC (NHC = N-Heterocyclic Carbene) Complexes: A Reliable, User-Friendly, Highly Active Palladium Precatalyst for the Suzuki−Miyaura Reaction. *Chem. − Eur. J.* **2006**, *12* (18), 4743−4748.
(57) Webb, J. D.; Seki, T.; Goldston, J. F.; Pruski, M.; Crudden, C. M. Selective functionalization of the mesopores of SBA-15. *Microporous Mesoporous Mater.* **2015**, *203*, 123−131.
(58) Fihri, A.; Cha, D.; Bouhrara, M.; Almana, N.; Polshettiwar, V. Fibrous Nano-Silica (KCC-1)-Supported Palladium Catalyst: Suzuki Coupling Reactions Under Sustainable Conditions. *ChemSusChem* **2012**, *5* (1), 85−89.
(59) Ziegler, F.; Teske, J.; Elser, I.; Dyballa, M.; Frey, W.; Kraus, H.; Hansen, N.; Rybka, J.; Tallarek, U.; Buchmeiser, M. R. Olefin Metathesis in Confined Geometries: A Biomimetic Approach toward Selective Macrocyclization. *J. Am. Chem. Soc.* **2019**, *141* (48), 19014−19022.
(60) Yeh, Y. Q.; Lin, H. P.; Tang, C. Y.; Mou, C. Y. Mesoporous silica SBA-15 sheet with perpendicular nanochannels. *J. Colloid Interface Sci.* **2011**, *362* (2), 354−366.

https://doi.org/10.1021/acs.macromol.3c00870
Macromolecules XXXX, XXX, XXX−XXX